Multiple Neutral Loss Monitoring (MNM): A Multiplexed Method for Post-Translational Modification Screening

Michael D. Hoffman,* Matthew J. Sniatynski, and Jason C. Rogalski
The Biomedical Research Centre, University of British Columbia, Vancouver, British Columbia, Canada

J. C. Yves Le Blanc
MDS Sciex, Concord, Ontario, Canada

Juergen Kast
Department of Chemistry, University of British Columbia, Vancouver, British Columbia, Canada

Post-translational modifications of proteins are involved in determining the activity of proteins and are essential for proper protein function. Current mass spectrometric strategies require one to specify a particular type of modification, in some cases also a particular charge state of a protein or peptide that is to be studied before the actual analysis. Due to these requirements, most of the modifications on proteins are not considered in such an experiment and, thus, a series of similar analyses need to be performed to ensure a more extensive characterization. A novel scan strategy has been developed, multiple neutral loss monitoring (MNM), allowing for the comprehensive screening of post-translational modifications (PTM) on proteins that fragment as neutral losses in a mass spectrometer. MNM method parameters were determined by performing product ion scans on a number of modified peptides over a range of collision energies, providing neutral loss energy profiles and optimal collision energies (OCE) for each modification, supplying valuable information pertaining to the fragmentation of these modifications and the necessary parameters that would be required to obtain the best analysis. As the optimal collision energy was highly dependent on the type of modification and the charge state of the peptide, the MNM scan was operated with a collision energy gradient. Autocorrelation analyses identified the type of modification, and convolution mapping analyses identified the associated peptide. The MNM scan with the new collision energy parameters was successfully applied to a mixture of four modified peptides in a BSA digest. The implementation of this technique will allow for comprehensive screening of all modifications that fragment as neutral losses. (J Am Soc Mass Spectrom 2006, 17, 307–317) © 2006 American Society for Mass Spectrometry

Many researchers in proteomics are concerned with the analysis of low-abundance proteins as they tend to be regulatory proteins that are involved in environmental changes and cell signaling. Post-translational modifications are responsible for determining the activity of these proteins, and they are a very common mechanism employed by cells for regulating biological processes such as gene transcription and translation, apoptosis, anti-apoptosis, protein degradation, etc. [1]. There are over 300 different types of post-translational modifications [2], with each type of modification having one or more unique functions within the cell [3]. Identification of post-translational modifications is typically performed on triple quadrupole instruments using precursor ion scans on the charged marker ion or neutral loss scans on the characteristic uncharged fragments. A neutral loss scan is performed on a triple quadrupole instrument by scanning the ionized peptides or proteins through the first quadrupole (Q1). The ions are then fragmented in the second quadrupole (Q2) through low-energy collisions with a collision gas in the collision cell. The third quadrupole is then scanned with a fixed offset to Q1 specific to the modification and the charge state of the precursor peptide, transmitting the precursor ion minus the modification, i.e., the product ion of the neutral loss, to the detector [4]. This neutral loss analysis identifies the presence of a modification as well as the associated precursor ion; however, as this scan function requires that a quadrupole be scanned, the duty cycle is in the

Published online January 27, 2006

Address reprint requests to Dr. J. Kast, The Biomedical Research Centre, University of British Columbia, 2222 Health Sciences Mall, Vancouver, BC V6T 1Z3, Canada. E-mail: kast@brc.ubc.ca

* Also at the Department of Chemistry, University of British Columbia, Vancouver, BC, Canada.

1044-0305/06/$32.00
doi:10.1016/j.jasms.2005.11.002

Received August 24, 2005
Revised November 3, 2005
Accepted November 7, 2005

range of 0.1%, i.e., if a mass range of 1000 Th is scanned in 1 Th increments, only 1/1000 of the time is spent transmitting the ion to the collision cell. The duty cycle drops even lower if a quadrupole time-of-flight mass spectrometer is used for the identification of neutral losses [5]. This time-consuming process requires at least one analysis per post-translational modification, as one must specifically search for a particular modification from a peptide of some particular charge state. This limits the total number of modifications screened in LC-MS/MS experiments, especially considering their inverse relationship with sensitivity in a fixed time frame. As well, due to the poor duty cycle, the acquisition rate must be rather long and, thus, the neutral loss scan (as well as the precursor ion scan) is not routinely used for the analysis of subpicomole quantities of peptides by LC-MS [5]. For these reasons, a novel scan technique has been developed to overcome the limitations of the conventional methods used to monitor for post-translational modifications.

Methods

Reagents

The following peptides (bold amino acid residues indicate the site of modification) were obtained from the following sources: sulphated tyrosine (D**Y**MGWMDF) (Novabiochem, Darmstadt, Germany), phosphotyrosine (NRV**Y**IHPF), phosphoserine (**S**APPNLWAAQR), glycosylated serine (HLLV**S**NVGGDGEEIER) (gifts from BRC, Vancouver, British Columbia, Canada), oxidized methionine (HD**M**NKVLDL) (Sigma-Aldrich, St. Louis, MO). Bovine Serum Albumin (BSA) was purchased from Sigma-Aldrich. Sequencing grade trypsin was obtained from Roche Diagnostics (Laval, Quebec, Canada). Formic Acid, acetonitrile, ethanol, and trifluoroacetic acid were purchased from Fisher Scientific (Whitby, Ontario, Canada).

Mass Spectrometry

Method development was performed with peptides containing post-translational modifications at 5 μM in methanol/water/formic acid (50:45:5). Neutral loss collision energy profiling for the method development of the multiple neutral loss monitoring (MNM) scan was performed on a 2000 Q-TRAP instrument (Applied Biosystems/MDS Sciex, Framingham, MA) in nanospray mode using the enhanced product ion (EPI) scan, which essentially traps all product ions utilizing Q3 as a linear ion trap [6]. Neutral loss collision energy profiles of all neutral losses were collected by varying the collision energy from 5 to 150 eV in increments of 2 V for the collision energy acceleration potential. For each neutral loss, three neutral loss collision energy profiles were collected and then averaged.

A new scan was developed to be able to perform multiple neutral loss monitoring, which allowed Q1 to be used as a high mass filter (set with a low mass cut off of m/z 350). This cut off was selected to eliminate the low mass background of the solvent [5, 8]. Acceleration voltages of 10, 15, 20, 25, and 30 V were applied from Q0 to Q2 to fragment the transmitted peptides in Q2. The peptides were trapped in Q3, and then sequentially scanned out. Analysis of complex samples was performed at submicromolar concentrations of the modified peptide alone or spiked into a Bovine Serum Albumin (BSA) digest producing a standard mixture of approximately 250 femtomoles of modified peptides in a 250 femtomole BSA digest in 1% formic acid. The BSA digest was prepared by reducing, alkylating, and digesting the BSA overnight using sequencing grade trypsin [7]. Both analyses were performed on the 2000 Q-TRAP with an Ultimate nano-HPLC (LC Packings, Sunnyvale, CA, USA) using the MNM scan. HPLC separations used water:acetonitrile:formic acid with gradient elution. All scans were collected with a scan speed of 1000 u/s.

Computational Analyses

Resulting LC-MS/MS spectra were analyzed using correlation analyses. A threshold was applied to each mass spectrum that was three times the noise intensity, ensuring that only peaks that were at least three times the signal to noise ratio were analyzed. This routinely produced mass spectra that contained 4 to 12 peaks. An autocorrelation analysis was then performed on the entire MNM spectrum to identify apparent mass shifts that corresponded to known neutral losses. Eq 1 was used for the autocorrelation analysis:

$$r = \frac{\sum_{i=a}^{b} [(X_{1i} - X_{1M})(X_{2(i-d)} - X_{2M})]}{[\sum_{i=a}^{b} [(X_{1i} - X_{1M})^2]^{1/2} [\sum_{i=a}^{b} (X_{2(i-d)} - X_{2M})^2]^{1/2}} \quad (1)$$

r = correlation coefficient
X_{1i} = intensity of Spectrum 1 at m/z i
X_{1M} = mean intensity of Spectrum 1
$X_{2(i-d)}$ = intensity of copy of Spectrum 1 at m/z i-d
X_{2M} = mean intensity of copy of Spectrum 1
d = apparent mass shift
a = data acquisition start position (Th)
b = data acquisition stop position (Th)

In the autocorrelation analysis, the position in the mass spectrum (i) is fixed and the apparent mass shift (d) is varied so as to allow the copy of the mass spectrum (2) to be shifted incrementally down the entire mass spectrum (1), providing correlations seen in the apparent mass shift which would correspond to different neutral losses. The correlation coefficient (r) was plotted against the apparent mass shift (d) to identify the neutral loss.

A convolution mapping analysis using this mass shift was applied to the mass spectrum, which identi-

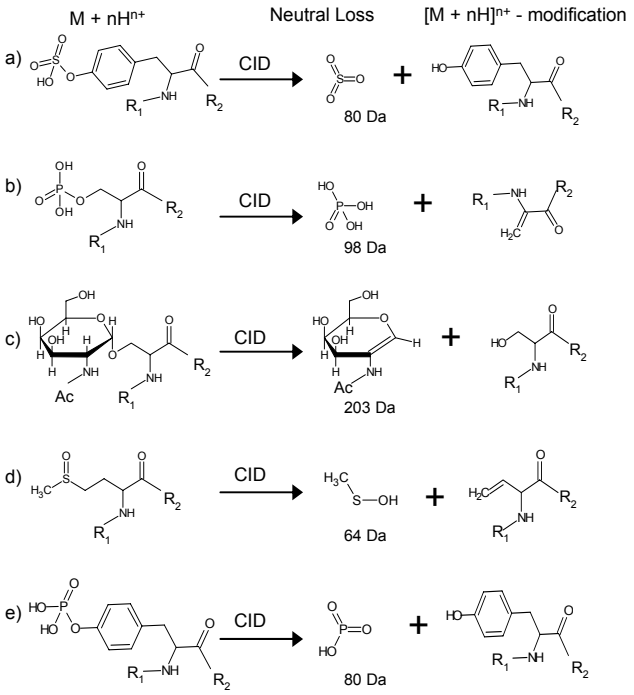

Figure 1. The structure of the precursor ions, neutral losses and product ions, as well as the corresponding neutral loss mass for (**a**) sulfotyrosine, (**b**) phosphoserine, (**c**) N-acetylhexosamine-modified serine, (**d**) oxidized methionine, and (**e**) phosphotyrosine.

fied the precursor ion. Eq 2 was used for the convolution mapping analysis:

$$c = [(X_{1i} - X_{1M})(X_{2(i-d)} - X_{2M})] \quad (2)$$

c = convolution mapping coefficient

In the convolution mapping analyses, the apparent mass shift (d) is fixed, while the position in the mass spectrum (i) is varied in fixed increments (e.g., 0.077 Th). This can be pictured as having a window with width d (e.g., d of 49 for the neutral loss of H_3PO_4 which is lost from a doubly-charged phosphoserine-modified peptide) shifted along the mass spectrum in increments of 0.077 Th. The intensity of the two peaks that lie on the window edges are then multiplied together to produce a convolution mapping coefficient (c) for every value of (i). The convolution mapping coefficient was plotted against the position (i) in the mass spectrum. The precursor ion was identified as the maximum in the convolution mapping analysis.

Results and Discussion

Method Design

Modified peptides tend to fragment to either produce a characteristic marker ion or neutral fragment from the precursor ion. As both these marker ions and neutral fragments generally have unique mass increments, they are used to indicate the presence of some modification. The structure of the precursor ion ($[M + nH]^{n+}$), neutral

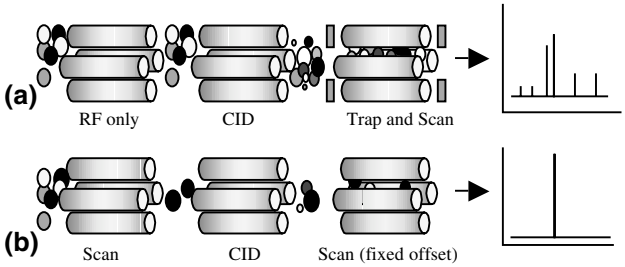

Figure 2. Mass analyzer configuration and corresponding characteristic mass spectra for (**a**) the multiple neutral loss monitoring (MNM) scan and (**b**) the neutral loss scan.

loss fragment and its mass increment, as well as the associated product ion ($[M + nH - modification]^{n+}$) for a number of different modifications that were used in this study are illustrated in Figure 1. Specifically, these modified residues are sulfotyrosine (Figure 1a), phosphoserine (Figure 1b), N-acetylhexosamine modified-serine (Figure 1c), oxidized methionine (Figure 1d), and phosphotyrosine (Figure 1e).

Utilizing the unique trapping capabilities of a hybrid triple quadrupole/linear ion trap, we previously demonstrated the ability to rapidly identify multiple marker ions with the development of multiple precursor ion monitoring (MPM) [8]. MPM is performed by transmitting all peptides through Q1 to the collision cell, then fragmenting them in parallel. The resulting low mass fragment ions are trapped in Q3, then scanned out and detected, identifying the presence of modifications. This scan function increases the duty cycle to 100%; however, due to constraints of the linear quadrupole ion trap, the extraction efficiency is 20% [9]. Current research with linear ion traps has been investigating the possibilities of increasing this extraction efficiency [10], but the 20% extraction efficiency still equates to a theoretical 200-fold sensitivity increase compared to the neutral loss scan. MNM is an analogous method to MPM; however, only the high mass fragments are scanned out of Q3, thus producing a mass spectrum that contains both the modified peptide and the peptide where the modification has been lost as a neutral fragment (Figure 2a). In contrast, as the neutral loss scan function scans both the first and third quadrupole (Figure 2b), the precursor ion minus the modification is the only ion to be registered at the detector, identifying both the precursor ion and the modification. Unfortunately, the neutral loss scan is limited to one charge state of one type of modification, while the MNM scan can detect multiple neutral losses regardless of the charge state of the precursor ion.

With the mass spectrum obtained from the MNM scan, further downstream computer processing is required to identify the neutral loss and the associated precursor ion; thus, an autocorrelation analysis is conducted to identify the neutral loss from the precursor ions (Figure 3a and b). A copy of the mass spectrum (Figure 3a) is created and is overlaid on top of the

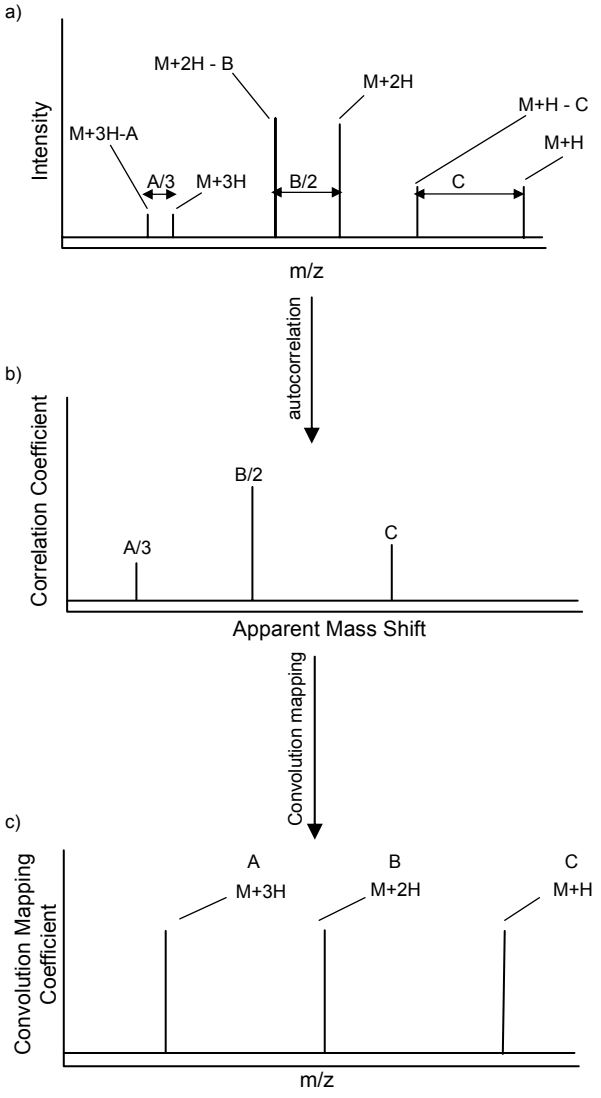

Figure 3. Theoretical steps of the data processing of MNM, consisting of (**a**) an MNM mass spectrum, (**b**) the resulting autocorrelation analysis identifying the neutral loss(es), and (**c**) the corresponding convolution mapping analysis identifying the associated precursor ion(s).

original mass spectrum. The top mass spectrum is then shifted incrementally to lower *m/z* values. Theoretically, at a very small mass shift, none of the peaks of the top spectra will be directly overlaid on any of the peaks on the bottom spectra. This is not the case in a real analysis, as the background will always be overlaid on real peaks, and thus to simplify the autocorrelation analysis, a threshold is applied to the mass spectrum to remove the background and low intensity peaks. At some mass shift, one of the peaks from the top spectrum (i.e., M + 3H) will be overlaid on one of the peaks from the bottom mass spectrum (i.e., M + 3H - A) corresponding to a mass shift of some modification (i.e., modification A) divided by the charge state of the peptide (i.e., 3). Similarly, a mass shift of B/2 is seen when M + 2H is overlaid on M + 2H - B and a mass shift of C is seen when M + H is overlaid on M + H - C. These mass shifts of A/3, B/2 and C are then plotted in the autocorrelation analysis (Figure 3b), identifying all of the neutral losses corresponding to all of the different types of modifications that are present in the sample from all of the different charge states of the peptide. With the mass shift (and thus the modification) identified, it is possible to identify the precursor ion. A convolution mapping analysis is applied to the mass spectrum (Figure 3a) using the identified mass shift (Figure 3b). A window with a width equal to the modification- and charge state-specific mass shift (i.e., A/3, B/2, C) detected in the autocorrelation is moved incrementally up the mass spectrum. When both peaks fall on the edges of the window, a large convolution mapping coefficient is produced, identifying the precursor ion (Figure 3c). Thus, this analysis is capable of identifying both the modification and precursor ion of every modification that fragments as a characteristic neutral loss from all of the charge states of that peptide. This analysis does not use time-correlation of the elution profiles to identify the precursor and product ions as this is done by the convolution mapping analysis; however, with a high-resolution chromatographic separation, comparison of the precursor and product ion elution profiles could be used to confirm the identification. Furthermore, a high-resolution liquid chromatographic separation would allow for a quantitative proteomic analysis as previously shown by accurate mass retention time pairs [11] or protein correlation profiling [12], although nonlinearity of the signal response and ion suppression effects may be a concern.

Method Development

MNM scans of a serine-glycosylated peptide spiked into a BSA digest were acquired at a collision energy of 30 eV (Figure 4a), followed by the autocorrelation analysis of the spectrum (Figure 4c) to identify the neutral loss and then the convolution mapping analysis (Figure 4e) to identify the associated precursor ion. The autocorrelation analysis of the glycosylated serine modification is fairly uncomplicated by random noise as only 4 peaks are observed in the autocorrelation plot. The peak at a mass shift of 101.5 Th corresponds to the loss of the glycosyl moiety (203 Da) from a doubly-charged peptide, but a number of additional, seemingly unrelated correlations were also identified. The convolution mapping analysis reveals the *m/z* of the precursor ion (964 Th) as the only signal, and no false positives were identified. A similar set of experiments for a phosphorylated tyrosine peptide spiked into a BSA digest were conducted with MNM scans at a collision energy of 30 eV (Figure 4b), an autocorrelation analysis (Figure 4d), and a convolution mapping analysis (Figure 4f). The autocorrelation analysis of the phosphoserine-modified peptide contains a fair degree of noise and spurious peaks. The peak at an apparent mass shift of 49 Th corresponds to the loss of phosphoric acid (98 Da) from a doubly-charged precursor ion. The convo-

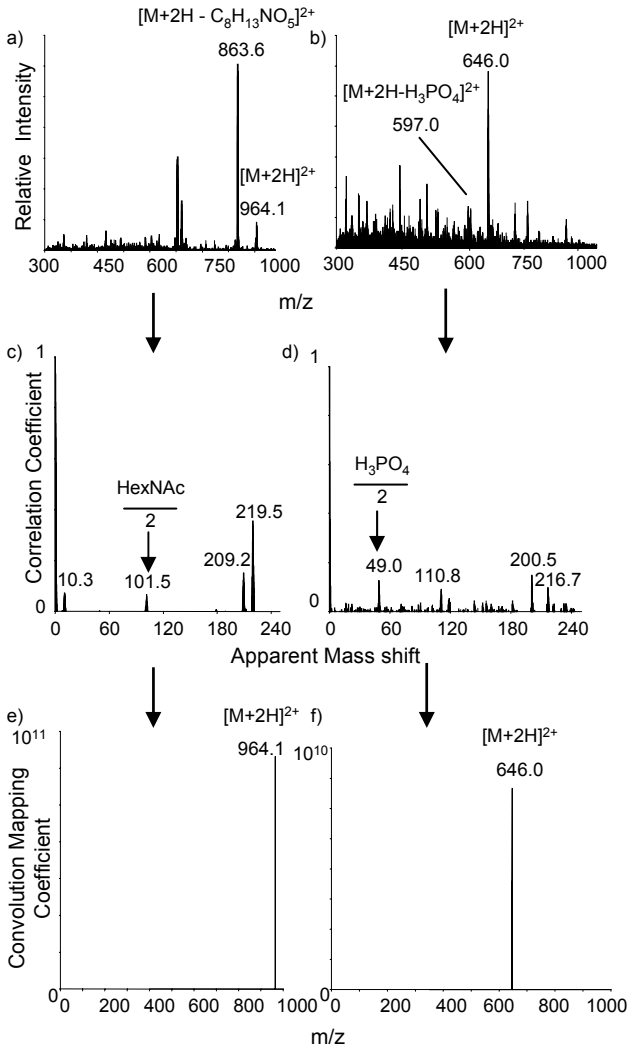

Figure 4. MNM scans using an acceleration potential of 15 V (**a**) and (**b**), corresponding autocorrelation (**c**) and (**d**), and convolution mapping analyses (**e**) and (**f**), of 250 femtomoles of N-acetylhexosamine-modified serine peptide spiked into 250 femtomoles of BSA digest (**a**), (**c**), and (**e**) and 250 femtomoles of phosphoserine-modified peptide spiked into 250 femtomoles of BSA digest (**b**), (**d**), and (**f**).

lution mapping successfully identifies the precursor ion at 646 Th, and no other precursor ions were identified as there was only one peak. The noise and the peaks that do not correspond to a neutral loss seen in the autocorrelation are dependent on the threshold used on the mass spectrum before the autocorrelation. The greater the number of peaks within the threshold-applied mass spectrum, the greater the noise and the number of peaks observed in the autocorrelation analysis. The peaks that do not correspond to a characteristic neutral loss for post-translational modifications are the result of two or more signals that are separated by this specific mass to charge ratio. There are three possibilities of how these peaks are generated. The first possibility is that the *m/z* difference corresponds to the removal of individual amino acid residues as is commonly observed for fragment ion series of the same charge state such as the y- and b- type ions at higher collision energies. The second possibility is for these spurious peaks to be due to the *m/z* difference corresponding to the removal of several amino acid residues due to the presence of labile bonds, e.g., N-terminal of proline. The direction of the *m/z* shift is then dependent on the distribution of the charges on the fragments and results in a "neutral loss" of a peptide fragment, or two fragment ions [13–15]. The neutral loss of individual amino acid residues has previously been observed [13, 14]. These studies have shown that low collision energies can lead to the formation of neutral fragments carrying the first or first two residues from the peptide, and that certain amino acids are much more likely to cleave as a neutral loss, depending on the charge state of the peptide. In both of these cases, as the *m/z* differences observed between these fragment ions correspond to the masses of amino acid residues and characteristic neutral losses of post-translational modifications have unique mass shifts that do not usually correspond to these amino acid residue masses, this does not tend to be a problem for the analysis. As subsequent analyses would only be performed on characteristic neutral losses, these peaks are of little importance; however, as the number of spurious peaks decreases, the probability of a random peak occurring at a mass shift corresponding to a neutral loss of interest also decreases. In this context, a combination of low resolution of the quadrupole and isotopic peaks could also lead to the false identification of a modification. This is observed for the neutral loss of a farnesyl moiety from a doubly-charged precursor ion (shift of 102.0 Th) that is incorrectly identified as a neutral loss of an N-acetylhexosamine moiety from a doubly-charged precursor ion (shift of 101.5 Th) (data not shown). Upon examination of the autocorrelation data, the maximum correlation was identified at 102.0 Th with 101.5 Th being a lower intensity satellite signal; thus, this false positive could be identified, explained, and excluded. False identifications caused by the neutral loss of amino acid residues (e.g., the neutral loss of 97, 98, and 99 Da for proline, phosphoric acid, and valine, respectively) would be dealt with in a similar manner. Ultimately, the ability of the autocorrelation data to distinguish these interferences will increase with the mass resolution of the instrument. The third possibility for these peaks is due to the *m/z* charge difference between two completely independent signals, either attributable to fragmentation or the coelution of several peptides. These correlations are completely random and cannot be predicted. In the case of the coelution of several peptides, the method benefits from a high quality liquid chromatographic separation.

Since only four of the peaks within the glycosylated serine MNM mass spectrum (Figure 4a) were above the threshold, the autocorrelation analysis is very simple. Conversely, the autocorrelation analysis of the serine-phosphorylated peptide is complicated by a large num-

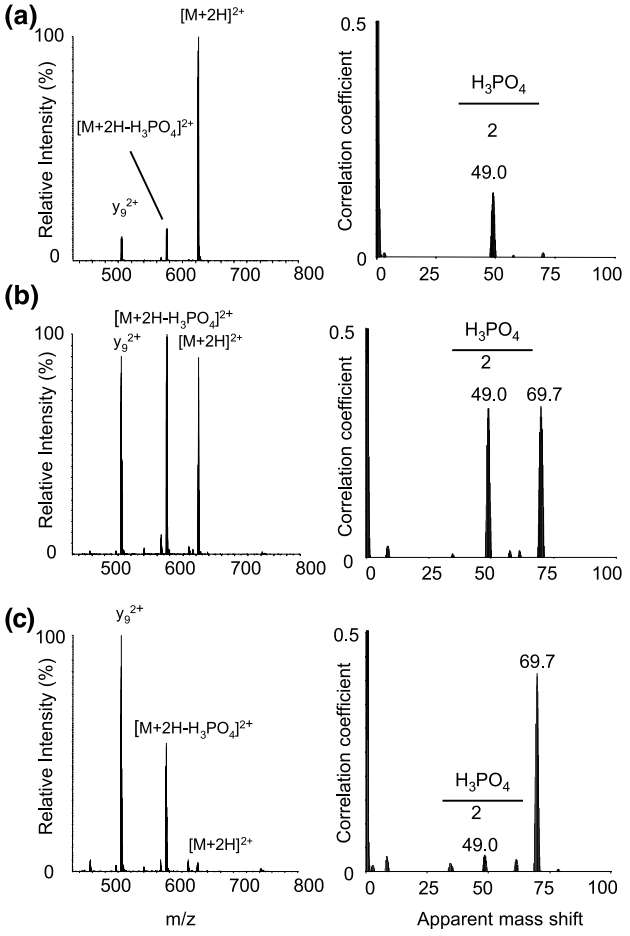

Figure 5. Enhanced product ion (EPI) mass spectra of a phosphorylated serine-modified peptide (**S**APPNLWAAQR) at a collision energy of (**a**) 30 eV, (**b**) 46 eV, and (**c**) 60 eV, and the corresponding autocorrelation analyses.

ber of peaks with low intensity. This is due to the higher number of signals above the noise. Upon examination of the mass spectrum (Figure 4b), it is evident that if the intensity of the $[M + 2H - H_3PO_4]^{2+}$ product ion increases relative to the rest of the peaks in the spectrum, this condition will lead to an increase in the correlation. Thus, to obtain the highest possible number for the correlation coefficient, a ratio of 1:1 of the precursor ion to the precursor ion minus the modification is useful. This 1:1 ratio can be obtained by varying the collision energy applied to the peptide in the collision cell and will be referred to as the optimal collision energy (OCE). Therefore, tight control of the collision energy provides a means of excluding false positives generated by the three possibilities mentioned earlier, as well as its use will lead to the highest possible correlation value.

Enhanced product ion spectra of the phosphoserine-modified peptide were collected over a wide range of collision energies. At low collision energies (Figure 5a), the abundance of the intact peptide is much greater than the peptide minus the modification. At these low energies, the precursor ion has a low kinetic energy and upon collision with the collision gas in Q2, the peptide will not be very likely to fragment as its energy is below the threshold for fragmentation of the bond that connects the modification to the peptide side chain. The corresponding autocorrelation only contains the peak corresponding to the neutral loss of a mass shift of 49 Th; however, the correlation coefficient of 0.14 is not maximal. At some moderate collision energy (Figure 5b), the two ions have the same abundance as the precursor ion fragments to produce product ions. The autocorrelation analysis describes the presence of two peaks of equal intensity; one from a correlation from the y_9^{2+} fragment ion and the precursor ion minus the modification at 69.7 Th and one corresponding to the neutral loss. The correlation coefficient for the neutral loss has increased to 0.33 and the analysis contains very little noise. At higher collision energies (Figure 5c), the peptide minus the modification becomes the dominant species out of the two ions. At these higher collision energies, significant backbone fragmentation of the peptide occurs which would complicate the autocorrelation analysis. This complication is seen in the autocorrelation analysis as a number of peaks are now present. As well, the correlation coefficient corresponding to the phosphoric acid neutral loss has significantly decreased to 0.04. It is evident that the largest correlation coefficient is obtained when the ratio of precursor ion to precursor ion minus the modification approaches one. In this 1:1 case, if these were the only two signals in the mass spectrum, the correlation coefficient would have a maximum value of 0.5. However, with increased collision energies, significant backbone fragmentation also occurs, exemplified by the formation of the y_9^{2+}, which causes additional signals to appear in the spectra and reduces the correlation coefficient for the peak at an apparent mass shift of 49 Th, which was due to the loss of phosphoric acid. Regardless, this 1:1 ratio is still desirable. Based on these results, it is also evident that a higher collision energy is required for the MNM scan of the phosphoserine-modified peptide compared to the 30 eV previously used (Figure 4a) while a collision energy below 30 eV is required for the MNM scan of the serine-glycosylated peptide (Figure 4b).

Consequently, the dependence of collision energy on the production of modification specific neutral losses was investigated for a number of different modifications as well as for different charge states, when possible. The results are summarized in Figure 6 using two different types of plots, with the structures of the corresponding precursor ions and fragments seen in Figure 1. Neutral loss intensity profiles are plots of the intensity of the precursor ion and the product ion at varying collision energies, while the neutral loss ratio profiles are plots of the ratio of the precursor ion : product ion and product ion : precursor ion. These two ratios have been plotted in the cases when the favorable 1:1 ratio can be obtained as it allows one to visualize that only a narrow collision energy range (~12 to 15 eV) corresponds to a ratio

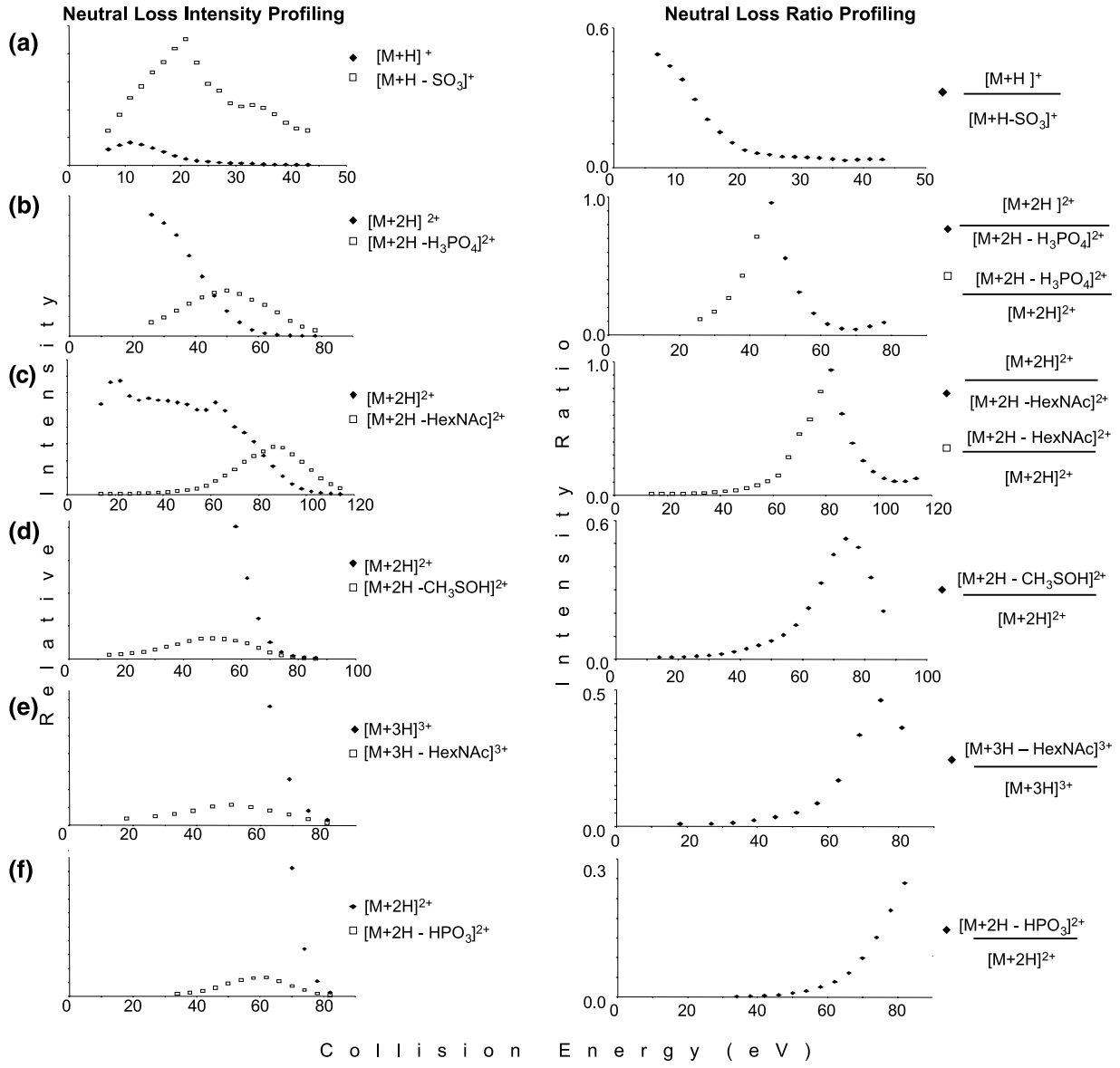

Figure 6. Neutral loss intensity profiling and neutral loss ratio profiling of peptides containing post-translational modifications. (**a**) Sulfotyrosine, (**b**) phosphoserine, (**c**) N-acetylhexosamine (doubly-charged), (**d**) oxidized methionine, (**e**) N-acetylhexosamine (triply-charged), and (**f**) phosphotyrosine.

between 0.5 to 1. Only one of the ratios is plotted in the remainder of the cases, for which this 1:1 ratio is not reached. As the sulfotyrosine modification is very labile, even at very low collision energies, the M + H - SO_3 product ion is the dominant species compared to the precursor ion (Figure 6a). As the total ion transmission is low at very low acceleration potentials, the OCE is 11 eV for the sulfotyrosine. This would also be the optimal collision energy for the neutral loss scan as this is the apex of the product ion intensity profile, but the product ion is the dominant species and 1:1 ratio is not obtained. For the phosphoserine (Figure 6b) and the doubly-charged N-acetylhexosamine-modified serine (Figure 6c) containing peptides, the OCE is 45 and 81 eV, respectively, as seen when the ratio of M + 2H : M + 2H minus the modification approaches 1 in the neutral loss ratio profile as well as by the intersection point in the neutral loss intensity profiles. In both examples, the precursor ion does not tend to fragment at low collision energies. Increasing the collision energy, the precursor ion begins to fragment to give the neutral loss. Further increasing the collision energy produces the 1:1 ratio of the precursor ion to the product ion (precursor ion minus the modification). Increasing the collision energy a few eV results in a maximum in the product ion neutral loss intensity profile, which would be the optimal collision energy for the neutral loss scan. Continuing to increase the collision energy, both the precursor ion and product ion intensity decreases as both ions are fragmented. As

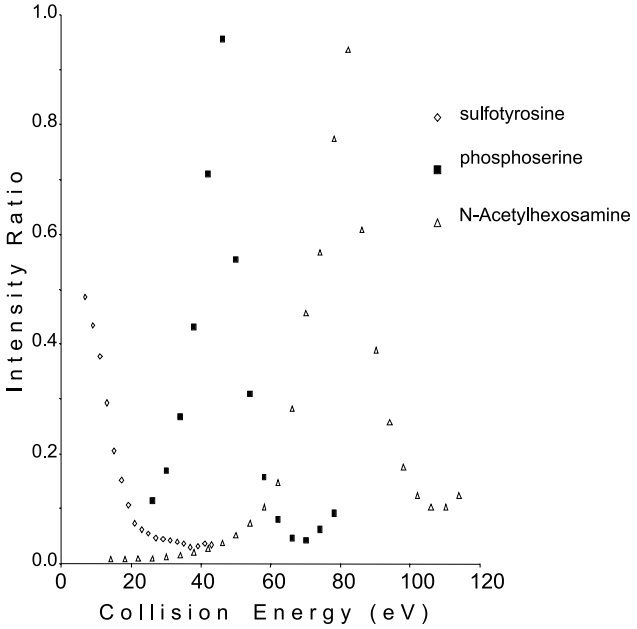

Figure 7. Optimal collision energy reference graph for three labile post-translational modifications: Sulfotyrosine, phosphoserine, and N-acetylhexosamine-modified serine.

expected from Figure 4, the OCE for the serine-phosphorylated peptide is above 30 eV; however, the OCE for the glycosylated serine is also above 30 eV when it was expected to be below 30 eV based on Figure 4. The reason for this is that in the MNM scan all charge states of the peptide are transmitted through the first quadrupole. As the triply-charged peptide fragments to produce mainly the marker ions, it also produces the doubly-charged peptide minus the modification, in addition to the unfragmented triply-charged peptide and the triply-charged peptide minus the modification. Therefore, the doubly-charged peptide minus the modification in Figure 4a is the sum of the fragment ions generated from doubly- and triply-charged species. Thus, its intensity is higher than when the doubly-charged precursor ion is isolated in Q1 as was done in Figure 6. The oxidized methionine (Figure 6d), triply-charged N-acetylhexosamine-modified serine (Figure 6e) and phosphotyrosine (Figure 6f) containing peptides do not tend to fragment to give a large abundance of the peptide minus the modification, and fail to produce a 1:1 ratio, so the OCE has been reached when the signal of the peptide minus the modification is at a maximum at 50, 51, and 60 eV, respectively. It should be noted that the triply-charged glycosylated serine tends to produce very little of the neutral loss compared to the doubly-charged precursor ion. Instead, it fragments to produce known modification-specific marker ions [16], which was also the case with the doubly-charged phosphotyrosine modification [17].

As seen here with peptides, there is an optimal collision energy for each modified peptide where the intensity of the modified peptide is equal to the intensity of the peptide where the modification has fallen off. This concept of an optimal collision energy has previously been shown for glycosides using a neutral loss scan and thus they recommended the use of a collision energy gradient [18]. A similar procedure was proposed for PTM marker ion monitoring with a stepped collision energy approach [19]. When the neutral loss collision energy profiles of several modifications are combined into a single reference graph (Figure 7), it becomes evident that a collision energy gradient is necessary for the MNM scan function as each modification has a unique optimal collision energy dependent on the type of modification and charge state of the peptide. More importantly, at the optimal collision energy of the phosphoserine modification, neither of the other modifications would be identified since one is completely fragmented (sulfotyrosine) and the other has not yet begun to fragment (N-acetylhexosamine).

Schlosser and coworkers have previously shown for phosphorylated peptides that the optimal collision energy is also (linearly) dependent on the size of the peptide [20]. Therefore, only the development of the MNM scan with a collision energy gradient would allow for the collection of mass spectra at each optimal collision energy, producing the most statistically significant autocorrelation interpretation. Implementing the collision energy into the MNM scan further improves the selectivity of the analysis if a false positive occurs due to a random correlation. In any case, false positives will not be analyzed if this correlation is seen at some collision energy that does not correspond to the characteristic collision energy for that neutral loss. Thus, implementing collision energy as a key parameter in the development of the MNM scan will lead to a much more selective analysis given that peptide mass, charge state, and sequence are also taken into account. Therefore, operating this scan with a collision energy gradient would also facilitate the analysis of multiple modifications on a single peptide. Multiple modifications of the same type are easily identified at their optimal collision energy as the autocorrelation analysis would report multiples of a given modification-specific mass shift (e.g., 2×49 Th = 98 Th for a doubly-charged, doubly-phosphorylated peptide), and the subsequent convolution mapping analysis would identify the origin of the single and multiple mass shifts. In contrast, multiple modifications of different types can only be identified in a sequential fashion, as the mass shift of the more labile modification would be detected at a low collision energy, and that of the more stable modification at high collision energy in the autocorrelation. However, sequential convolution analysis would still identify one as the product of the other as the product ion of the first neutral loss is only transient and not present in the lowest collision energy spectra.

Since the collision energy is defined as the collision energy acceleration potential multiplied by the charge state of the peptide, it is impractical to operate the MNM scan with an actual collision energy as we are transmitting

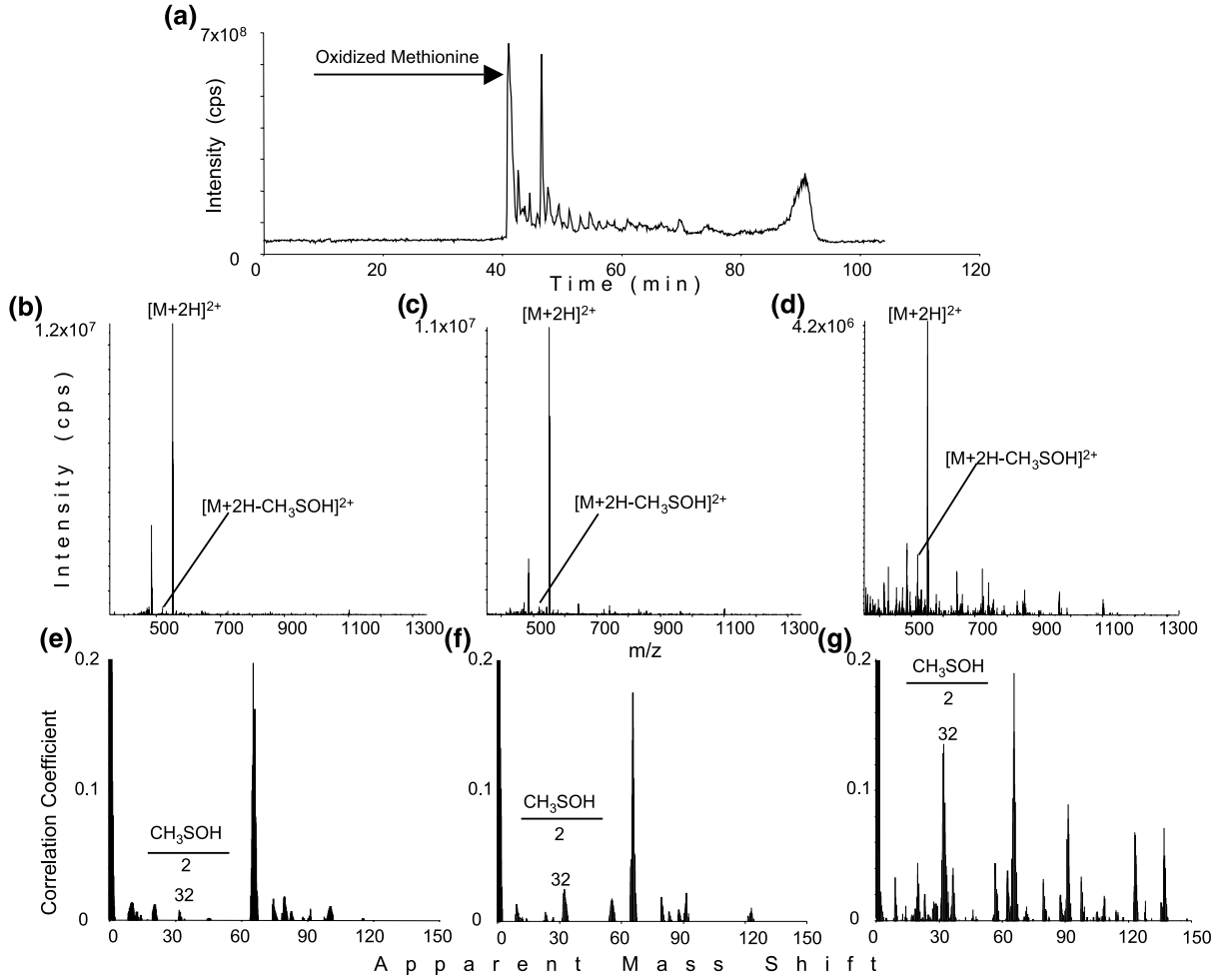

Figure 8. MNM analysis of 250 femtomoles of an oxidized methionine-containing peptide in 250 femtomoles of a BSA digest taken at collision energy acceleration potentials of 10, 20, and 30 V. (**a**) Total ion chromatogram with the corresponding MNM mass spectrum of the oxidized methionine containing peptide at a collision energy acceleration potential of (**b**) 10 V, (**c**) 20 V, and (**d**) 30 V, and the corresponding autocorrelation analysis at (**e**) 10 V, (**f**) 20 V, and (**g**) 30 V.

precursor ions of different charge states through the mass analyzer. Thus, we will use the optimal collision energy acceleration potential when referring to the optimal collision energy, which is 11, 22, 40, 25, 17, and 30 V for the six different species, in the order used in Figure 6. Furthermore, as seen in the neutral loss ratio profiles for the modifications that fragment to give the 1:1 ratio, as well as the neutral loss intensity profile for the sulfotyrosine and the stable modifications, the scan should be operated with the collision energy increasing in increments of 5 V. Increments of greater than 5 V may not identify the modification as the analysis may occur outside of the optimal range. The use of a collision energy gradient with increments smaller than 5 V will lead to too much time being spent fragmenting the precursor ion outside of the optimal collision energy range. Therefore, it was concluded that testing of the MNM scan should be performed at 5 different acceleration potentials 10, 15, 20, 25, and 30 V. The maximum acceleration potential was set to 30 V because as the collision energy increases, the degree of backbone fragmentation dramatically increases and this would complicate the autocorrelation analysis.

Method Evaluation

The MNM analysis of an oxidized methionine-containing peptide in a BSA digest was carried out to illustrate the importance of the collision energy gradient (Figure 8). Investigation of the autocorrelation analysis and MNM mass spectrum at a collision energy acceleration potential of 10 V indicates that very little of the precursor ion minus the modification has been formed, which is why the correlation coefficient for the autocorrelation signal at 32 Th is very low. At a collision energy acceleration potential of 20 V, the intensity of the $[M + 2H - CH_3SOH]^{2+}$ peak has increased in intensity in the MNM spectrum leading to an increase in the value of the correlation coefficient. At a collision energy acceleration potential of 30 V, the intensity of the $[M + 2H - CH_3SOH]^{2+}$ peak has increased again in the MNM

spectrum as has the correlation coefficient; however, the number of spurious peaks has also increased dramatically. Therefore, the analysis of this peptide is best performed between 20 and 30 V, which is in agreement with the optimal collision energy acceleration potential that was determined to be 25 V in Figure 6.

The selectivity of the MNM scan was tested by mixing four modified peptides (N-acetylhexosamine, oxidized methionine, phosphoserine and sulfotyrosine) creating a 500 femtomoles per microliter mixture in 0.1% formic acid and then loading 500 femtomoles on column. Indeed, all four peptides were detected in a single MNM experiment (data not shown). These four peptides were then spiked into a BSA digest and were successfully identified from a more complex biological matrix that mimicked an enzymatic digest of a modified protein (Figure 9). The mixture was analyzed at five different collision energy acceleration potentials, and each of the five corresponding total ion chromatograms showed the presence of a large number of peptides (Figure 9a). The total ion chromatogram that corresponded to the OCE for each modification was then used to extract the MNM spectrum at every time point, and an autocorrelation of each MNM spectrum was performed. The autocorrelation coefficient corresponding to the apparent mass shift of the neutral loss was then collected from each of the autocorrelation analyses, which allowed for the construction of an extracted ion chromatogram of autocorrelation coefficients. Figure 9b is a composite of the four extracted ion chromatogram autocorrelation coefficients, which is then followed by a convolution mapping analysis (Figure 9c) that was collected at the time corresponding to the autocorrelation coefficient maxima. This identified the precursor ions responsible for the apparent mass shifts identified in Figure 9b. The peaks at 36.6 and 77.3 min in Figure 9b were attributed to oxidized methionine as the mass spectra showed a mass shift of 32 (64 for the loss of CH_3OH divided by a charge state of 2). The peaks at 40.7, 42.4, and 45.2 min were attributed to the N-acetylhexosamine modification as the mass spectra showed a mass shift of 101.5 (203 for the loss of the N-acetylhexosamine moiety divided by a charge state of 2). The peak at 49.5 min was attributed to phosphoserine due to an apparent mass shift of 49 (98 for the loss of H_3PO_4 divided by a charge state of 2) and the peaks at 54.9 and 77.0 min were attributed to sulfotyrosine due to an apparent mass shift of 80 (80 for the loss of SO_3 divided by a charge state of 1). The subsequent convolution mapping analysis (Figure 9c) identified the modified precursor ions that were associated with the apparent mass shifts. The peak at 36.6 min was successfully identified as the oxidized methionine peptide as it had a *m/z* of 550.7 Th. The other peak that was identified as an oxidized methionine containing peptide is a false positive that is due to the correlation of the singly-charged sulfotyrosine modified peptide minus the sulfo moiety and some other ion. In the analysis of the glycosylated peptides, the peak at 40.7 min was

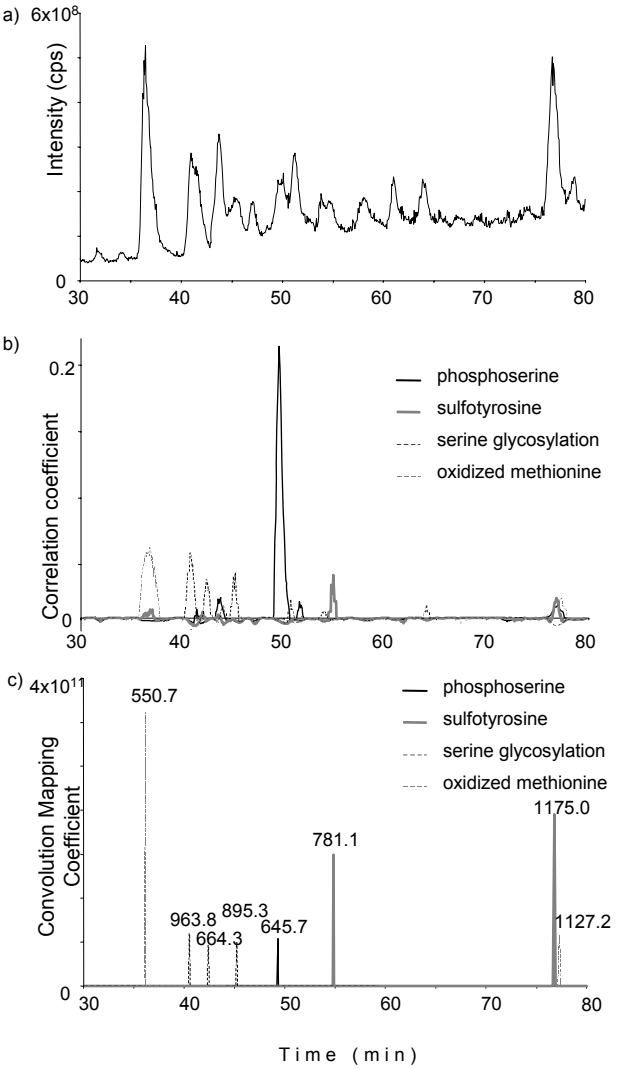

Figure 9. MNM analysis of a mixture of serine glycosylated, oxidized methionine, (1 picomole each), sulfotyrosine, and phosphoserine (2 picomoles each) modified peptides in a 250 femtomole BSA digest. (**a**) Total ion chromatogram at a collision energy acceleration potential of 10 V, (**b**) overlayed reconstructions of the extracted ion chromatograms autocorrelation coefficients of the apparent neutral losses of sulfotyrosine at 10 V, glycosylated serine at 20 V, phosphoserine at 25 V, oxidized methionine at 25 V, and (**c**) convolution mapping analysis identifying the modified precursor ions.

successfully identified as being serine glycosylated as it had a *m/z* of 963.8 Th, while the two other peaks at 42.4 and 45.2 min were identified as false positives. The peak at 49.5 min was successfully identified as the phosphoserine containing peptide as it had a *m/z* of 645.7 Th and the peak at 77.0 min was identified as the singly-charged sulfotyrosine containing peptide with a *m/z* of 1175.0. The peak at 54.9 min was identified as a false positive. All four of the modified peptides were successfully identified by this analysis with very few false positives identified. In any case, as all of the false positives were associated with some peptide within the sample, further analysis of these peptides would still yield valuable information.

Conclusions

The multiple neutral loss monitoring (MNM) scan function successfully identified a number of different modifications that may not have been identified in a neutral loss scan unless each modification was specifically monitored. The MNM scan has thus been shown to be a very powerful method for comprehensive post-translational modification monitoring. Further investigation of the dependence of the optimal collision energy on the peptide size, charge state, and sequence are required to better define their relationships, which could be fashioned into an algorithm to facilitate the MNM scan. Applications of the MNM scanning method for the complete analysis of protein and protein complexes from biological matrices will be the next step.

Acknowledgments

This work was funded in part by operating grants from the Canadian Institutes of Health Research (CIHR) and the Protein Engineering Network of Centers of Excellence (PENCE). MDH thanks the Natural Sciences and Engineering Research Council (NSERC) for a CGS scholarship. The authors thank Phil Owen for the donation of peptides.

References

1. Sechi, S. Mass spectrometric approaches to quantitative proteomics. In *Contributions to Nephrology* Thonyboonkerd, V.; Klein, J. B.; Eds.; Karger Publishers: Switzerland, 2004; pp 59–78.
2. http://www.abrf.org/index.cfm/dm.home. *Delta mass—A database of protein post translational modifications*; 2005.
3. Mann, M.; Jensen, O. N. Proteomic analysis of post-translational modifications. *Nat. Biotechnol.* **2003,** *21,* 255–261.
4. Covey, T.; Shushan, B.; Bonner, R.; Shroder, W.; Hucho, F. LC/MS and LC/MS/MS screening for the sites of post-translational modification in proteins. Jornvall, H.; Hoog, J. O.; Gustavsson, A. M., Eds.; In *Methods of protein sequence analysis*; Birkhauser Verlag: Basel, Germany, 1991; pp 249–256.
5. Bateman, R. H.; Carruthers, R.; Hoyes, J. B.; Jones, C.; Langridge, J. I.; Millar, A.; Vissers, J. P. C. A novel precursor ion discovery method on a hybrid quadrupole orthogonal acceleration time-of-flight (Q-TOF) mass spectrometer for studying protein phosphorylation. *J. Am. Soc. Mass Spectrom.* **2002,** *13,* 792–803.
6. Hager, J. W.; Le Blanc, J. C. Y. Product ion scanning using a Q-q-Qlinear ion trap (Q TRAP) mass spectrometer. *Rapid Commun. Mass Spectrom.* **2003,** *17,* 1056–1064.
7. Park, Z. Y.; Russell, D. H. Thermal denaturation: A useful technique in peptide mass mapping. *Anal. Chem.* **2000,** *72,* 2667–2670.
8. Rogalski, J. C.; Lin, S.; Kast, J. Multiple precursor ion monitoring—a new scan strategy on hybrid quadrupole/linear ion trap mass spectrometers? *Rapid Commun. Mass Spectrom.* **2004,** *18,* 739–741.
9. Hager, J. W. A new linear ion trap mass spectrometer. *Rapid Commun. Mass Spectrom.* **2002,** *16,* 512–526.
10. Moradian, A.; Douglas, D. J. Axial ion ejection from linear quadrupoles with added octopole fields. *Proceedings of the 53rd ASMS Conference on Mass Spectrometry and Allied Topics*; San Antonio, TX, June 2005.
11. Silva, J. C.; Denny, R.; Dorschel, C. A.; Gorenstein, M.; Kass, I. J.; Li, G. Z.; Mckenna, T.; Nold, M. J.; Richardson, K.; Young, P; Geromanos, S. Quantitative proteomic analysis by accurate mass retention time pairs. *Anal. Chem.* **2005,** *77,* 2187–2200.
12. Andersen, J. S.; Wilkinson, C. J.; Mayor, T.; Mortensen, P.; Nigg, E. A.; Mann, M. Proteomic characterization of the human centrosome by protein correlation profiling. *Nature* **2003,** *426,* 570–574.
13. Salek, M.; Lehmann, W. D. Neutral loss of amino acid residues from protonated peptides in collision-induced dissociation generates N- or C-terminal sequence ladders. *J. Mass Spectrom.* **2003,** *38,* 1143–1149.
14. Martin, D. B.; Eng, J. K.; Nesvizhskii, A. I., Gemmill, A.; Aebersold, R. Investigation of neutral loss during collision-induced dissociation of peptide ions. *Anal. Chem.* **2005,** *77,* 4870–4882.
15. Rogalski, J. C.; Lin, M. S.; Sniatynski, M. J.; Taylor, R. J.; Youhnovski, N.; Przyblyski, M.; Kast, J. Statistical evaluation of electrospray tandem mass spectra for optimized peptide fragmentation. *J. Am. Soc. Mass Spectrom.* **2005,** *16,* 505–514.
16. Rogalski, J. C.; Kast, J. Specific detection of O-linked N-acetylhexosamine modified peptides using multiple precursor ion scans. *Rapid Commun. Mass Spectrom.* **2005,** *19,* 77–78.
17. Steen, H.; Küster, B.; Fernandez, M.; Pandey, A.; Mann, M. Detection of tyrosine phosphorylated peptides by precursor ion scanning quadrupole TOF mass spectrometry in positive ion mode. *Anal. Chem.* **2001,** *73,* 1449–1454.
18. Qu, J.; Liang, Q.; Luo, G.; Wang, Y. Screening and identification of glycosides in biological samples using energy-gradient neutral loss scan and liquid chromatography tandem mass spectrometry. *Anal. Chem.* **2004,** *76,* 2239–2247.
19. Bean, M. F.; Annan, R. S.; Hemling, M. E.; Huddleston, M. J.; Carr, S. A. LC-MS methods for selective detection of posttranslational modifications in proteins: Glycosylation, phosphorylation, sulfation, and acylation. In *Techniques in Protein Chemistry*, Vol. VI.; Crabb, J. W., Ed.; Academic Press: New York, 1995; pp 107–116.
20. Schlosser, A.; Pipkorn, R.; Bosseymeyer, D.; Lehmann, W. D. Analysis of protein phosphorylation by a combination of elastase digestion and neutral loss tandem mass spectrometry. *Anal. Chem.* **2001,** *73,* 170–176.